U.P.B. Sci. Bull., Series A, Vol. 75, Iss. 1, 2013 ISSN 1223-7027

BEHAVIOURS OF FLUIDIZED BEDS THROUGH FLOW REGIMES OF A COMPLEX FLUID

Irina-Elena SURDU[1], Carmen NEJNERU[2], Gelu GĂLUŞCĂ[3], Maricel AGOP[4,]

Comportamentele de păturilor fluidizate prin regimuri de curgere diferite ale unui lichid complex sunt analizate. Simulările numerice arată că fluidizarea este un proces de tranziție continuu. Mai mult decât atât, multe tipuri de faze fluidizate ca faze omogene sau faze amestecuri sunt modelate. Faza corespunde unui regim de curgere specific, în timp ce fluidizarea este asociată unor instabilități convective.

The behaviours of fluidized beds through the different flow regimes of a complex fluid are analyzed. Numerical simulations show that the fluidization is a continuous transition process. Moreover, many types of fluidized phases as homogeneous, channeling, bubbling phases or mixtures phases are mimed. The phase corresponds with a specific flow regime, while the fluidization is associated with convective instabilities.

Keywords: biphasic fluid, convective instabilities, fluidization, fluidized bed

1. Introduction

Fluidized beds consist of granular particles confined in a tall chamber with distributer for the fluid flow at the bottom [1-8]. In experiments injection of the energy in a system is controlled by the flow rate of fluid (we note that, since the granular materials are dissipative injection of the energy is necessary to preserve steady states). At low flow rate, the system is in the fixed phase where particle rest at the bottom. When the flow rate exceeds the critical value, the particles start moving. This state is called the fluidized phase, which contains sub-phases, for

[1] PhD. eng. Technical University Gh Asachi Iasi, Faculty of Science and Engineering Materials, Romania
[2] Lecturer, Technical University Gh Asachi Iasi, Faculty of Science and Engineering Materials, Romania
[3] Professor, Technical University Gh Asachi Iasi, Faculty of Science and Engineering Materials, Romania
[4] Professor, Technical University Gh Asachi Iasi, Faculty of Machine Manufacturing and Industrial Management, Department of Physics, Romania and Lasers, Atoms and Molecules Physics Laboratory, University of Science and Technology, Villeneuve d'Ascq, 59655, Lille, France

instance, the homogeneous phase, the bubbling phase, the channeling phase, etc [9].

There are many models to describe fluidized beds (two-fluid models, particle-dynamics models, etc). In the two-fluid models, the particles are treated as a fluid [10-13, 15, 17]. These models benefit by analytical treatments [22]. However, their bases, such as stress tensor and constitution equations for the particle-phase pressure have not been established. The particle-dynamics models describe the direct motion of the particles. There are various models which are kinetic theories [2], the discrete element method [23, 24] etc. These models cannot be the basis for the two-fluid models. Their main problem is that hydrodynamic interactions among particles are over simplified. For instance, the boundary conditions between particles and fluid are not satisfied in the scale of particles, and the fluid equation is calculated under inviscid limit.

A numerical model on the fluidized beds has been proposed in [9] where hydrodynamic interaction among particles is calculated with reliable accuracy. From its simulation, it results both the fact that fluidization is a continuous transition and that the two type of fluidized phases (the channeling phase and the bubbling one) exist. Also, close relations between the averaged behaviours in fluidized beds and quasi-equilibrium states in dense fluids are found. We note that by means of such simulation in fluidized beds, the flow rate plays the role of the effective temperature and existences of a kind of the fluctuation-dissipation relation are suggested.

According to our opinion, since in fluidized beds the interaction phenomena are of multi-scale type, dynamics in a complex fluid are practically analyzed in [9, 21, 25]. The homogeneous, the channeling and bubbling phase type cataloguing given by numerical simulations in [9, 25, 26] are not the best choices. In what follows, considering that a complex fluid (fluid + solid particle) is characterized by effective parameters, we numerical simulate the speed and temperature transfers for various flow regimes. These regimes will be assimilated to different fluid sub-phases (homogeneous, bubbling and channeling phases) or mixtures of fluidized beds sub-phases. Therefore, in what follows behaviours of fluidized beds through various flow regimes (speed and temperature fields) of a complex fluid will be mimed.

2. Specific parameters of a biphasic fluid

The biphasic fluid (fluid + solid particles) can work as a monophasic one, having effective fluid-phase parameters. In what fallows we shall define the effective parameters:

i) Effective density,

$$\rho = (1 - \varepsilon)\rho_f + \varepsilon\rho_p \quad (1)$$

where ρ_f is fluid density and ρ_p the density of the solid particle [1-3];

ii) Effective specific heat,

$$c = (1-\varepsilon)c_f + \varepsilon c_p \quad (2)$$

where c_f is the specific heat fluid and c_p is the specific heat of the solid particle [1-2];

iii) Effective thermal conductivity,

$$\lambda = \frac{\left[\lambda_p + (n-1)\lambda_f - (n-1)(\lambda_f - \lambda_p)\varepsilon\right]}{\left[\lambda_p + (n-1)\lambda_f + (\lambda_f - \lambda_p)\varepsilon\right]}\lambda_f \quad (3)$$

where λ_f is the thermal conductivity of the fluid, λ_p is the thermal conductivity of the particle and n is the empirical shape factor,

$$\mathrm{n} = {}^{3}/_{\psi} \quad (4)$$

where ψ is the ratio between the area of a sphere and the area of a particle having the same volume. Equation (3) specifies that the effective thermal conductivity is maximal for spherical particles. Furthermore, it ignores both particle size and radiation effect that can occur among particles [1-3];

iv) effective thermal expansion coefficient,

$$\alpha = (1-\varepsilon)\alpha_f + \varepsilon\alpha_p \quad (5)$$

where α_f is the coefficient of fluid thermal expansion and α_p is the solid particle thermal expansion coefficient [1-3];

v) Effective viscosity,

$$\eta = (306\varepsilon^2 - 0{,}19\varepsilon + 1)\eta_f \quad (6)$$

where η_f is fluid viscosity [1-2].

In relations (1), (2), (3), (5) and (6) ε correspond to particle volume fraction.

3. Convective instabilities in biphasic fluid

3.1. Convective instabilities phenomenology

Let us consider a biphasic fluid layer of thickness d subject to thermal gradient,

$$\beta = \frac{\Delta T}{d} = \frac{T_1 - T_0}{d} \quad (7)$$

where $\Delta\mathrm{T} = \mathrm{T}_1 - \mathrm{T}_0 < 0$ is the temperature difference between upper and lower borders of biphasic fluid layer. The pure conduction regime with the biphasic fluid at rest and undisturbed temperature distribution belongs to the thermodynamic branch continuously correlating the non-equilibrium state ($\Delta\mathrm{T} \neq 0$) with the balanced one($\Delta\mathrm{T} = 0$).

Let us examine the dynamics of temperature fluctuations, θ, in the vicinity of unperturbed temperature profile $T_0(z)$. Let us also consider an element of biphasic fluid with a higher temperature as compared to that of the environment, θ> 0. Density decreases with temperature, so the biphasic fluid element is lighter than any of its vicinities, with the tendency to rise. Heating the biphasic fluid in its inferior part, its density will increase with the altitude, so that the item meets an increasingly colder biphasic fluid, tending to increase faster and faster. The initial fluctuation is amplified. Two dissipative processes tend to maintain the biphasic fluid at rest:

- internal friction (the damping of the motion through viscosity);
- thermal conduction that reduces the temperature difference between the average element biphasic fluid and the environment, thus reducing buoyancy.

Instability cannot develop unless biphasic fluid element is accelerated enough to overcome the effect of dissipative processes. Temperature gradient β, which represents the control parameter of this instability, exceeds the critical value β_C.

An organized structure of convection cells type is generated above the critical limit.

3.2. Biphasic fluid dynamic equations

For a biphasic fluid, the mass, momentum and internal energy equations are:

$$\frac{\partial\rho}{\partial t}+\nabla\cdot(\rho\vec{v})=0$$
$$\frac{\partial(\rho\vec{v})}{\partial t}+\nabla\cdot\left(\overleftrightarrow{P}+\rho\vec{v}\vec{v}\right)=\rho\vec{g} \tag{8 a-c}$$
$$\frac{\partial(\rho\varepsilon)}{\partial t}+\nabla\cdot\left(\rho\varepsilon\vec{v}+\vec{J}_q\right)=-\overleftrightarrow{P}:(\nabla\vec{v})$$

where ρ is the mass density of the biphasic fluid , $\vec{v}$ is its speed, $\vec{g}$ is the gravitational acceleration, ε is the internal energy of unit volume and $\vec{J}_q$ is the heat flux. Pressure tensor was noted with $\overleftrightarrow{P}$ and $\overleftrightarrow{A}:\overleftrightarrow{B}=A_{ic}B_{ci}$ the tensor product where Einstein's mute index summing convention (summing according to the repeated indices) was considered. Pressure tensor can be written as:

$$\overleftrightarrow{P}=\overleftrightarrow{P}^e+\overleftrightarrow{P}^v \tag{9}$$

where $\overleftrightarrow{P}^e$ is the balanced part depending on the state system and $\overleftrightarrow{P}^v$ is the non-balanced one corresponding to viscous pressure tensor. When balanced, viscous stress tensor components are null for an isotropic fluid at rest

$$\overleftrightarrow{P}^e=\begin{pmatrix}p&0&0\\0&p&0\\0&0&p\end{pmatrix}=p\overleftrightarrow{I} \tag{10}$$

where p is the hydrostatic pressure while for a non-balanced viscous biphasic fluid, the viscous stress tensor is not null. Now, according to relations (8) and (9), the pressure tensor for a balanced homogeneous and isotropic viscous biphasic fluid will be:

$$\overleftrightarrow{P} = p\overleftrightarrow{I} + \overleftrightarrow{P}^{v} \tag{11}$$

3.3 Constraints in biphasic fluid dynamics. Simplified dynamic equations

Let us admit the following assumptions:

i) The biphasic fluid is assumed Newtonian, a case in which the pressure tensor is given by equation (10). The viscous stress tensor is:

$$P^{\mathrm{v}}_{\alpha\beta} = -\xi(\nabla\cdot\vec{\mathrm{v}})\delta_{\alpha\beta} - \eta\left[\frac{\partial \mathrm{v}_\alpha}{\partial x_\beta} + \frac{\partial \mathrm{v}_\beta}{\partial x_\alpha} - \frac{2}{3}(\nabla\cdot\vec{\mathrm{v}})\delta_{\alpha\beta}\right] \tag{12}$$

where ξ is the volume viscosity, and η is the tangential one (shear);

ii) Fourier type thermal conduction

$$\vec{J}_q = -\lambda\nabla T \tag{13}$$

where λ is the effective thermal conductivity;

iii) Thermal expansion is linear

$$\rho = \rho_0[1 - \alpha(T - T_0)] \tag{14}$$

where α is the effective thermal expansion coefficient;

iv) The biphasic fluid satisfies caloric equation of state,

$$\bar{\varepsilon} = cT \tag{15}$$

where c is the heat capacity of unit volume of the biphasic fluid at constant pressure;

v) Thermal expansion of the biphasic fluid is small. Then we can consider the effective density everywhere constant, and denote it with ρ_0, except for the momentum balance equation.

Given these assumptions and using the method from [27, 28], the system of equations (8a-c) becomes:

$$\begin{gathered}\nabla\cdot\vec{\mathrm{v}} = 0\\ \rho_0\left[\frac{\partial\vec{\mathrm{v}}}{\partial t} + (\vec{\mathrm{v}}\cdot\nabla)\vec{\mathrm{v}}\right] + \nabla\mathrm{p} = (\rho_0 + \delta\rho)\vec{g} + \eta\Delta\vec{\mathrm{v}}\\ \frac{\partial T}{\partial t} + (\vec{\mathrm{v}}\cdot\nabla)T = \frac{\lambda}{\rho_0 c}\Delta T\end{gathered} \tag{16a-c}$$

where ρ is the effective perturbed density

$$\rho = \rho_0 + \delta\rho \tag{17}$$

Equation (16a) specifies that the biphasic fluid should be incompressible.

The convection in the layer of biphasic fluid releases when the buoyancy generated by thermal expansion is stronger than viscous forces. The Rayleigh number results

$$\mathcal{R} = \frac{|\vec{F}_{asc}|}{|\vec{F}_{\text{vâsc}}|} \approx \frac{\left|\frac{\delta\rho\vec{g}}{\rho_0}\right|}{\left|\frac{\eta\Delta\vec{v}}{\rho_0}\right|} \tag{18}$$

The explicit dependence of the Rayleigh number must take into account the following:

i) the effective density perturbation satisfies through (14) the relationship

$$\frac{\delta\rho}{\rho_0} \approx \alpha\Delta T \tag{19}$$

ii) from the internal energy balance equation (16c), relationship

$$\text{v} \approx \frac{\lambda}{\rho_0 c}\frac{1}{d} \tag{20}$$

is found. Substituting (19) and (20) in (18), for the Rayleigh number we obtain:

$$\mathcal{R} = \frac{\alpha\beta\rho_0^2 cg}{\eta\lambda}\text{d}^4 \tag{21}$$

or more, taking into account (1)-(6),

$$\mathcal{R} = \text{g}\beta\text{d}^4\frac{[(1-\varepsilon)\alpha_f+\varepsilon\alpha_p][(1-\varepsilon)c_f+\varepsilon c_p][(1-\varepsilon)\rho_f+\varepsilon\rho_p]^2}{\eta_f\lambda_f(306\varepsilon^2-0{,}19\varepsilon+1)\frac{[\lambda_p+(n-1)\lambda_f-(n-1)(\lambda_f-\lambda_p)\varepsilon]}{[\lambda_p+(n-1)\lambda_f+(\lambda_f-\lambda_p)\varepsilon]}} \tag{22}$$

In convection, the control parameter is the Rayleigh number (22) mainly "manipulated", by the temperature gradient β.

3.4. Reference state and perturbations in biphasic fluid dynamics. Dynamic equations for perturbations.

We choose the reference stationary state condition $\vec{v}_s = 0$, for which equations (16b) and (16c) become:

$$\nabla p_s = -\rho_s g\hat{z} = -\rho_0[1-\alpha(T_s - T_0)]g\hat{z}$$
$$\Delta T_s = 0 \tag{23 a,b}$$

where $\hat{z}$ is the unit vector of vertical direction. We believe that pressure and temperature will only vertically vary. For temperature, boundary conditions are

$$T(x,y,0) = T_0;\ T(x,y,d) = T_1 \tag{24}$$

Integrating equation (23b) with these boundary conditions, the vertical temperature profile in reference state, will be linear

$$T_s = T_0 - \beta z \tag{25}$$

Substituting (25) in (23a) and integrating, we obtain:

$$p_s(z) = p_0 - \rho_0 g\left(1 + \frac{\alpha\beta z}{2}\right) z \tag{26}$$

The system condition depends on η and λ kinetic coefficients that appear in equations (16a-c). We study the stability of the reference state through the small perturbations method. The perturbation state is characterized by relations

$$\begin{aligned} \mathrm{T} &= T_s(z) + \theta(\vec{r}, t) \\ \rho &= \rho_s(z) + \delta\rho(\vec{r}, t) \\ \mathrm{p} &= p_s(z) + \delta p(\vec{r}, t) \\ \vec{\mathrm{v}} &= \delta\vec{\mathrm{v}}(\vec{r}, t) = (u, \mathrm{v}, w) \end{aligned} \tag{27a-d}$$

As shown in (27a-d), perturbation are time and position dependant. Substituting (27a-d) in equations (16a-c) and taking into account (25) and (26), we obtain, in linear approximation, the following equations for perturbations:

$$\begin{aligned} &\nabla \cdot \delta\vec{\mathrm{v}} = 0 \\ &\frac{\partial\theta}{\partial t} = \beta w + k\nabla^2\theta \\ &\frac{\partial\delta\vec{\mathrm{v}}}{\partial t} = -\frac{1}{\rho_0}\nabla\delta p + \nu\nabla^2\delta\vec{\mathrm{v}} \\ &\qquad + g\alpha\theta\hat{z} \end{aligned} \tag{28a-c}$$

where $k = {}^{\lambda}/_{\rho_0 c}$ is the effective thermal diffusivity and $\nu = {}^{\eta}/_{\rho_0}$ is the effective kinematic viscosity.

3.5. Dynamic dimensionless equations of perturbation

Let us introduce dimensionless variables in the system (28a-c)

$$\vec{\xi} = \frac{\vec{\mathrm{r}}}{\mathrm{d}}, \ \tau = \frac{\mathrm{k}}{\mathrm{d}^2}\mathrm{t}, \ \vec{\mathrm{v}} = \frac{\mathrm{d}}{\mathrm{k}}\delta\vec{v}, \ \mathrm{P} = \frac{\mathrm{d}^2}{\rho_0\nu\mathrm{k}}\delta\mathrm{p}, \ \Theta = \frac{g\alpha d^3}{\nu\mathrm{k}}\theta \tag{29a-e}$$

It follows that the perturbations satisfy dimensionless equations:

$$\begin{aligned} &\mathcal{P}^{-1}\left(\frac{\partial\vec{\mathrm{v}}}{\partial\tau} + \vec{\mathrm{v}} \cdot \partial_{\vec{\xi}}\vec{\mathrm{v}}\right) = -\partial_{\vec{\xi}}P + \Theta\hat{\mathrm{z}} + \partial_{\vec{\xi}\vec{\xi}}\vec{\mathrm{v}} \\ &\frac{\partial\Theta}{\partial\tau} + \vec{\mathrm{v}} \cdot \partial_{\vec{\xi}}\Theta = \mathcal{R}w + \partial_{\vec{\xi}\vec{\xi}}\Theta \\ &\partial_{\vec{\xi}}\vec{\mathrm{v}} = 0 \end{aligned} \tag{30a-c}$$

where $\mathcal{P}$ is the Prandtl number

$$\mathcal{P} = \frac{\nu}{k} = \frac{\eta c}{\lambda} = \frac{\eta_f\left(306\varepsilon^2 - 0{,}19\varepsilon + 1\right)\left[(1-\varepsilon)c_f + \varepsilon c_p\right]}{\lambda_f \frac{\left[\lambda_p + (n-1)\lambda_f - (n-1)(\lambda_f - \lambda_p)\varepsilon\right]}{\left[\lambda_p + (n-1)\lambda_f + (\lambda_f - \lambda_p)\varepsilon\right]}} \tag{31}$$

3.6. Numerical simulation

It is difficult to obtain some analytical solutions of the system of equations (30a-c). That is why we will numerically integrate it through the Lattice Boltzmann (LB) method, using the Bhatnagar-Gross-Krook (BGK) model [27].

Numerical simulation using Mattlab programming mode (our adaptive version [28] of the software from [13, 15]) corresponds to different flow regimes of a biphasic fluid as specified by Nusselt's number [1, 2].

$$\mathcal{N} = \frac{\left(\mathrm{f}/_{8}\right)(\mathcal{R} - 1000)\mathcal{P}}{1 + 12{,}7\left(\mathrm{f}/_{8}\right)^{1/2}\left(\mathcal{P}^{2/3} - 1\right)} \qquad (32a,b)$$

$$\mathrm{f} = [0{,}79\ln(\mathcal{R}) - 1{,}64]^{-2}$$

Figures (1 a-e) show the numerical solutions (curves of equal speed and temperature) for $0{,}6 < \mathcal{N} < 3{,}5$. An entire scenario for the evolution of convective instabilities will sequentially result: initiation for $\mathcal{N} < 0{,}7$, extension for $0{,}7 < \mathcal{N} < 1{,}6$ and generation of convection patterns for $2{,}9 < \mathcal{N} < 3{,}2$.

Assimiling the different flow regimes of the complex fluid with fluidization it results that this is a continuous transition process. That, many type of fluidized phases are presented: homogeneous phase for $\mathcal{N} < 0{,}7$, channeling phase for $0{,}7 < \mathcal{N} < 1{,}6$ and bubbling phase for $2{,}9 < \mathcal{N} < 3{,}2$. Moreover many mixture phase results: for example channeling - bubbling phase for $1{,}6 < \mathcal{N} < 2{,}9$, etc.

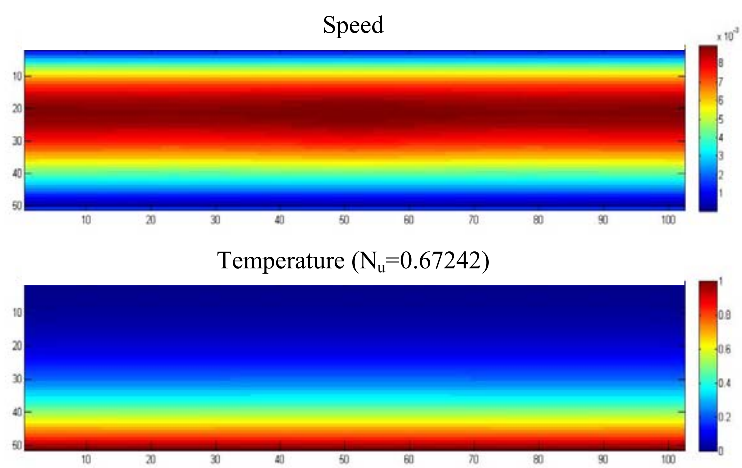

a)

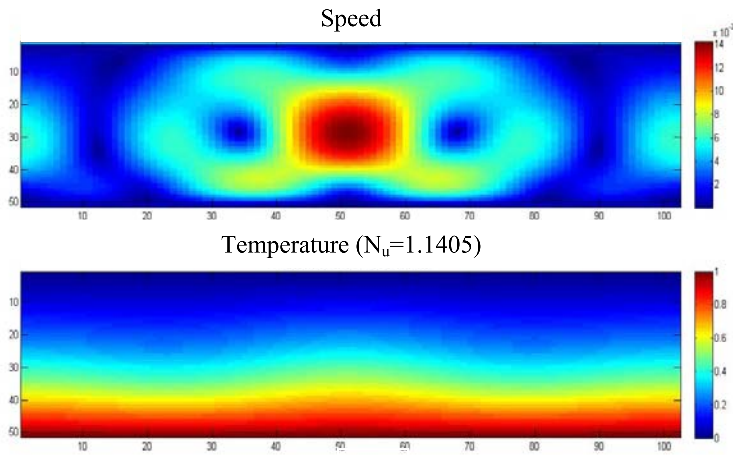
Speed
Temperature (N_u=1.1405)

b)

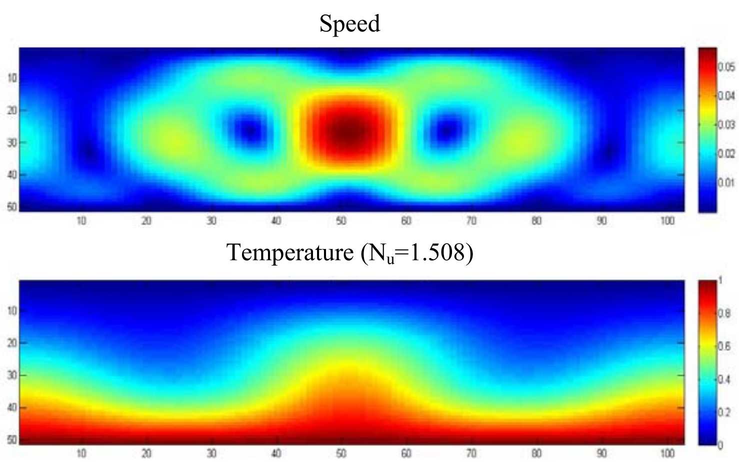
Speed
Temperature (N_u=1.508)

c)

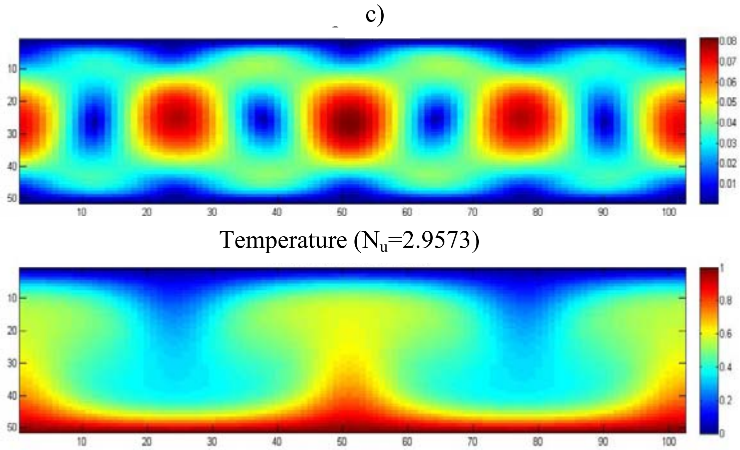
Temperature (N_u=2.9573)

d)

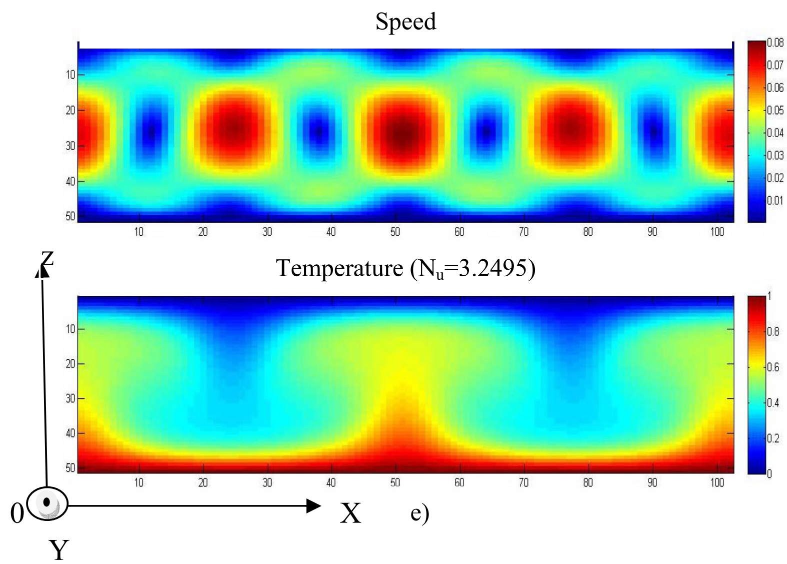

Figs. 1 (a-e) The numerical solutions (curves of equal speed and temperature) for 0,6 < $\mathcal{N}$ < 3,5.

Now, considering that the complex fluid is nitrogen gas and sand particles with the average parameters: ρ_f=1,2506 kg/m^3, ρ_p=3690 kg/m^3, c_f=1039,5 J/KgK, c_P=880 J/KgK, λ_f=0,02583 W/mK, λ_p=30 W/mK, η_f=0,0000152789, ε=1/3, n=21,86389 for a rotational ellipsoid (a=100 μm, b=300 μm, c=25 μm), β=12.500 K/m, d=0,8 mm, according with relation (32a,b), it results $\mathcal{N}$=*1,340212.* This means that a mixture phase (channeling – bubbling phase) in the fluidized beds appears. This result was confirmed by experiment [16,13].

4. Conclusions

The main conclusions of the present paper are follows: i) the behaviours of fluidized beds through the different flow regimes of a complex fluid are analyzed; ii) the complex fluid (fluid + solid particles) is characterized by effective parameters (effective density, effective specific heat, effective thermal conductivity, effective thermal expansion coefficient, effective viscosity); iii) various flow regimes through numerical simulations are mimed; it results that the fluidization is a continuous transition process. Moreover, many type of fluidized phases (homogeneous phase, channeling phase, bubbling phase, mixture phase) are presented; the each phase correspond with a specific flow regime, while the fluidization is associated with convective instabilities.

REFERENCES

[1] *Granular Matier* – An Interdisciplinary Approach – edited by A. Mehta, Springer-Verlag, New York, 1993
[2] *D. Gidaspow*, Multiphase Flow and Fluidization, Academic Press, London, 1994
[3] *J. F. Davidson, R. Clift and D. Harrison*, Fluidization, 2nd ed, Academic Press, London, 1985
[4] *C. Mihăilă*, Procese termodinamice în sisteme gaz solid şi aplicaţiile lor în industrie, Ed. Tehnică, Bucureşti, 1980
[5] *I. Grigoriu*, Reactoare chimice în strat fix şi fluidizat. Reactoare în strat fluidizat, Ed. Satya, Iaşi, 1998
[6] *Masayuki Horio*, Fluidizationscience, its development and future Elsevier, volume 8, issue 6, December 2010, Pages 514–524
[7] *Masayuki Horio,* Fluidization Past & Future , The 13th International Conference on Fluidization - New Paradigm in Fluidization Engineering, 2011
[8] *Kinshuk Dasgupta & co,* Formation of bamboo-shaped carbon nanotubes on carbon black in a fluidized bed, Journal of Nanoparticle Research ,Volume 14, Number 3 (2012), 728,:
[9] *K. Ichiki, H. Hayakawa*, arXiv: cond-mat/9704208v1 (cond-mat.stat mech), 25 Apr 1997
[10] *S. Sasa, H. Hayakawa*, Europhys Lett. 17, 685, 1992
[11] *M. F. Göz*, J. Fluid Mech. 240, 379, 1992
[12] *T. S. Komatsu, H. Hayakawa*, Phys Lett. A, 183, 56, 1993
[13] *JF de Jong, TYN Dang, M van Sint Annaland*, Comparison of a discrete particle model and a two-fluid model to experiments of a fluidized bed with flat membranes, Powder Technology, –Elsevier 2012
[14] *T Tsuji, K Higashid*, Numerical model for the motion of large object in fluidized bed, Bulletin of the American Physical Society, Volume 56, Number 18, 2011
[15] *A Bahramian,* Fluidization of micronic particles in a conical fluidized bed: Experimental and numerical study of static bed height effect, AIChE Journal, 2012 - Wiley Online Library
[16] *D Yang, Z Wang, X Huang, ,*Numerical Simulation on Superheated Steam Fluidized Bed Drying: I. Model Construction - *Drying Technology, 2011 - Taylor & Francis*
[17] *Q Wang, K Zhang,* CFD simulation of pressure fluctuation characteristics in the gas-solid fluidized bed: Comparisons with experiments- Petroleum Science, 2011 – Springer
[18] *S Shah, J Ritvanen, T Hyppänen…* Space averaging on a gas-solid drag model for numerical simulations of a CFB riser - Powder Technology, 2011 – Elsevier
[19] *XZ Chen, DP Shi, X Gao,* A fundamental CFD study of the gas–solid flow field in fluidized bed polymerization reactors - Powder Technology, 2011 - Elsevier
[20] *W Zhou, CS Zhao, LB Duan, CR Qu.*Two-dimensional computational fluid dynamics simulation of coal combustion in a circulating fluidized bed combustor - Chemical Engineering , 2011 - Elsevier
[21] *KW Chua, YT Makkawi,* Time scale analysis for fluidized bed melt granulation III: Binder solidification rate - Chemical Engineering Science, 2011 - Elsevier
[22] *T. S. Komatsu*, Phys. Rev. E, 52, 5574, 1995
[23] *Y. Tsuji, T. Tanaka, T. Ishida*, Powder Technology, 71, 239, 1992
[24] *Y. Tsuji, T. Kawaguchi, T. Tanaka*, Powder Technology, 77, 79, 1993
[25] *K. Ichiki, H. Hayakawa*, Phys. Rev E, 52, 658, 1995

[26] *OO Olaofe, MA Van der Hoef,* Bubble formation at a single orifice in a 2D gas-fluidized bed - Chemical Engineering …, 2011 - Elsevier
[27] *S. Chen, G. D. Doden*, Annual Review of Fluid Mechanics, 30, 329, 1998
[28] *A. Timofte, M. Agop*, Fractalitate şi nediferențiabilitate în dinamica fluidelor, Ars Longa, Iaşi, 2012